(12)

AD

US ARMY MATERIEL COMMAND

MEMORANDUM REPORT BRL-MR-3495

AD-A165 723

CONTACT SURFACE EROSION FOR HYPERVELOCITY PROBLEMS

Kent D. Kimsey
Jonas A. Zukas

February 1986

APPROVED FOR PUBLIC RELEASE; DISTRIBUTION UNLIMITED.

US ARMY BALLISTIC RESEARCH LABORATORY
ABERDEEN PROVING GROUND, MARYLAND

86 3 24 002

DISCLAIMER NOTICE

THIS DOCUMENT IS BEST QUALITY PRACTICABLE. THE COPY FURNISHED TO DTIC CONTAINED A SIGNIFICANT NUMBER OF PAGES WHICH DO NOT REPRODUCE LEGIBLY.

UNCLASSIFIED

SECURITY CLASSIFICATION OF THIS PAGE (When Data Entered)

REPORT DOCUMENTATION PAGE		READ INSTRUCTIONS BEFORE COMPLETING FORM
1. REPORT NUMBER Memorandum Report BRL-MR-3495	2. GOVT ACCESSION NO. AD-A165723	3. RECIPIENT'S CATALOG NUMBER
4. TITLE (and Subtitle) CONTACT SURFACE EROSION FOR HYPERVELOCITY PROBLEMS		5. TYPE OF REPORT & PERIOD COVERED Final
		6. PERFORMING ORG. REPORT NUMBER
7. AUTHOR(s) Kent D. Kimsey, Jonas A. Zukas		8. CONTRACT OR GRANT NUMBER(s)
9. PERFORMING ORGANIZATION NAME AND ADDRESS US Army Ballistic Research Laboratory ATTN: SLCBR-TB Aberdeen Proving Ground, MD 21005-5066		10. PROGRAM ELEMENT, PROJECT, TASK AREA & WORK UNIT NUMBERS 1L162618AH80
11. CONTROLLING OFFICE NAME AND ADDRESS US Army Ballistic Research Laboratory ATTN: SLCBR-DD-T Aberdeen Proving Ground, MD 21005-5066		12. REPORT DATE February 1986
		13. NUMBER OF PAGES 34
14. MONITORING AGENCY NAME & ADDRESS(if different from Controlling Office)		15. SECURITY CLASS. (of this report) UNCLASSIFIED
		15a. DECLASSIFICATION/DOWNGRADING SCHEDULE

16. DISTRIBUTION STATEMENT (of this Report)

Approved for public release; distribution unlimited.

17. DISTRIBUTION STATEMENT (of the abstract entered in Block 20, if different from Report)

18. SUPPLEMENTARY NOTES

This report is an expanded version of a paper presented at the 8th International Symposium on Ballistics, Orlando, FL, 1984.

19. KEY WORDS (Continue on reverse side if necessary and identify by block number)

Penetration Mechanics
Perforation
Ballistic Impact
Computer Simulation

20. ABSTRACT (Continue on reverse side if necessary and identify by block number)

This paper presents a technique for extending the capability of Lagrangian wave propagation codes to treatment of deep penetration and spaced plate perforation problems. Lagrangian codes as originally developed required that the sliding interfaces specified at the beginning of a problem remain unchanged throughout the computation. This requirement was imposed not from physical considerations but to simplify the programming of the interface logic. Its effect was to prohibit total failure of material dictated by the physical problem (i.e., front-face spall), resulting in either unrealistic distortions

DD FORM 1 JAN 73 1473 EDITION OF 1 NOV 65 IS OBSOLETE

UNCLASSIFIED

SECURITY CLASSIFICATION OF THIS PAGE (When Data Entered)

CONT.

of the computational grid leading to large truncation errors or minuscule temporal integration increments resulting in uneconomical computations. The contact surface erosion algorithm outlined in this paper permits sliding interfaces to be dynamically relocated as materials exceed their load-bearing capability without a prior specification of the damage region. Results obtained with EPIC-2 into which this algorithm has been incorporated show good agreement with experimental data for deep penetration situations as well as for finite plate perforations at striking velocities of 1.1 - 3.75 km/s.

TABLE OF CONTENTS

LIST OF ILLUSTRATIONS

PRECEDING PAGE BLANK

LIST OF TABLES

I. INTRODUCTION

The mechanics of penetration and perforation of solids has long been of interest for military applications and is currently being applied to a number of industrial applications such as the integrity of nuclear reactor pressure vessels, crashworthiness of vehicles, protection of spacecraft from meteoroid impact, and explosive forming and welding of metals.

Impacts at velocities in excess of 1 km/s excite the high frequency modes of the colliding solids. The response is confined to a localized region (typically 2 to 3 projectile diameters) and is characterized by the presence of shock waves and high hydrodynamic pressures which, on contact, can exceed the material strength by an order of magnitude. For ordnance velocity impacts (1-3 km/s) the pressures decay rapidly due to the presence of free surfaces and the effects of material strength and, except at the interface, oscillate at values comparable to the material strength. Under hypervelocity conditions (4-12 km/s), hydrodynamic pressure dominates the behavior of the solids for the bulk of the penetration process. Material strength effects become significant only in the very late stages of the process. Superimposed on these is extensive plastic deformation, large localized heating and material failure due to a number of mechanisms (i.e., petalling, spall, adiabatic shear). The failure mechanism(s) activated depend on geometry, loading history and material constitution. Strain rates of $10^5 s^{-1}$ at the impact interface and $10^2 - 10^3 s^{-1}$ elsewhere are not uncommon. Penetration and perforation are formidable physical problems and it is not surprising that the bulk of the research in this area has been experimental in nature.

A complete mathematical description of the dynamics of impacting solids must account for the geometry of the interacting bodies; elastic, plastic, and shock wave propagation; hydrodynamic flow, finite strains and deformations; thermal and frictional effects, and the initiation and propagation of failure in the colliding solids. During the past decade, rapid progress has been achieved in computational penetration mechanics.[1] Today, two- and three-dimensional simulations of high velocity impact phenomena, are routinely performed in conjunction with experimental studies in terminal ballistics.

Numerical simulation of penetration phenomena can be performed with both Lagrangian (mass reference) and Eulerian (laboratory reference) descriptions. In the laboratory reference scheme, the computational mesh remains stationary with material being transported through it based on velocity gradients present in the flow field. Such a description is ideally suited for modeling severe material deformations that occur in hypervelocity impacts, explosive-metal interactions and the penetration of thick targets (i.e., situations wherein the ratio of target thickness to penetrator diameter, t/D, exceeds 3). In the mass reference description the computational mesh is fixed in the material and distorts with it in accordance with applied loads. The Lagrangian approach offers the advantages of being conceptually straightforward (due to the lack of convective terms to represent mass flow) and permitting material boundaries to be delineated without ambiguity. However, irregular mesh shapes arising from severe material deformations lead to inaccuracies in the numerical approximation which can grow to unacceptable levels. In addition, since almost all Lagrangian wave propagation codes use explicit temporal integration schemes (in which the maximum time step is limited to satisfy a stability condition), violent distortion of the computational mesh leads to a reduction of the time step to such a low value that continuing the calculation becomes economically prohibitive. These problems can be overcome through the use of rezoning, coupled Lagrangian-Eulerian descriptions, and contact surface erosion algorithms.

In rezoning, a new Lagrange computational mesh is overlaid on the old one and a rezone algorithm maps mesh quantitites of the severely distorted mesh onto the new mesh such that conservation of mass, momentum, total energy and the constitutive relationship are satisfied. Rezoning can be a costly and nontrivial process. For very thick target penetration studies (plate thickness to projectile diameter ratios greater than 10) 30 to 50 rezones are not uncommon. Frequent rezoning renders the computational mesh semi-Eulerian in that large distortions are realized but material history and location of material boundaries are diffused.

Many impact situations are not simulated very well with Lagrangian or Eulerian descriptions alone (i.e., fluid-structure interaction problems). Coupling methodologies for combining Lagrangian and Eulerian descriptions exploit the respective advantages of each. In general, the Eulerian portion of the computational mesh behaves as a pressure boundary acting on the Lagrangian regions, while the Lagrangian regions represent obstacles in the Eulerian flow field. This technique does not circumvent the possibility of excessive diffusion of material history. While cumbersome and time-consuming logic for abating diffusion of material interfaces and histories have been demonstrated, the computational penalties for such logic are high.

A most promising technique to extend the capability of Lagrangian codes to deep penetration and spaced plate perforation problems is the concept of contact surface erosion. The Lagrangian codes developed in the seventies required that the contact surface or sliding interface specified at the beginning of the problem remain unchanged throughout. This requirement was imposed not from physical considerations but to simplify the interface logic. Its effect was to prohibit total failure of material dictated by the physical problem, resulting in either unrealistic distortions of the computational mesh leading to large truncation errors or to temporal integration increments which render further computation uneconomical.

The eroding contact surface concept has been under active investigation at a number of centers since 1978 and is now finding its way into production codes. The most comprehensive treatment is to be found in the DYSMAS/L code developed by Massmann, Poth and their associates at Industrieanlagen-Betriebsgesellschaft mbH (Ottobrun, W. Germany). The contact processor in DYSMAS/L [2-4] is based on a generalized master-slave concept. Structural surfaces which are to be controlled by the contact processor are defined as master planes and slave points. Both master surface erosion and internal cracking can be treated. In the case of element separation (crack opening) the separated nodal masses of the affected elements are designated as slave points to permit calculation of momentum exchange in case of further contact. Redefinition of the contact surface in case of erosion or cracking is treated automatically, requiring no user intervention.

Methods for dynamic redefinition of sliding interfaces in the presence of total element failure have also been developed by Johnson.[5 6] The earlier approach, implemented in the EPIC-3[5] code, had several limitations and restrictions (i.e., only obliquities of 45° or less could be treated and users had to specify a priori the extent of target damage) and has not been used extensively. Many of these have been removed from the techniques now used in current versions of EPIC-2 and EPIC-3. Snow[7] implemented logic to dynamically redefine the master surface as element failure occurs in the EPIC-2 code. The approach retained the requirement in the original version of the code that the master surface remain continuous and employed an asymmetric interface treatment. Most recently Belytschko[8] has introduced eroding contact surface concepts into the EPIC-3 code, making use of eight node hexahedral elements and hourglass viscosity to stabilize spurious deformation modes caused by one point integration.

II. CONTACT SURFACE EROSION FOR LAGRANGIAN COMPUTATIONS

Contact surfaces or sliding interfaces are appropriate in situations where large relative motions can be expected at material boundaries. Situations involving the interactions of gases and fluids with solid walls, the penetration of targets by projectiles, and contact between colliding bodies require the use of sliding interfaces. They prove useful also in regions where large shears or fractures develop. Most sliding interface methods are based on the decomposition of acceleration and velocity into components normal and tangential to the interface. Motions in the normal direction are continuous when materials are in contact but independent when they are separated. Tangential motions are independent when materials are separated or the interface is frictionless but are modified if there is contact and a frictional force is present. Materials on either side of an interface may separate if a user-specified criterion is exceeded or if materials are in tension, and may collide again if previously separated. A comprehensive discussion of sliding interface treatments is given by Hallquist.[9 10]

The sliding interface algorithm in the EPIC-2 code[7] has been restructured to simulate contact surface erosion during impact. Initially, a series of nodes lying on the interface are identified and labelled as either master or slave nodes. In the method employed here, a set of nodal points that define element edges or segments which have both nodes declared to be master nodes define unique master segments of the master surface on which slave nodes are not permitted to intrude. These master segments are not required to define the master surface in a continuous manner. When penetration of a slave node through the master surface occurs, the velocities of the master and slave nodes are adjusted to conserve angular and linear momentum as described in reference 11. Once the intrusions are removed, the designation of master and slave is interchanged and the procedure is repeated. Each temporal integration increment is comprised of the following steps:

1. Determine master segments, on one side of the interface, that circumscribes elements which have not exceeded the user specified failure criterion.

2. For each slave node, find the master segments which encompass the slave node within the search radius R which is ~ 0.6 of the length of the segment.

3. Once all segments associated with a given slave node have been located, determine if penetration of the segment has occurred. If only one segment is penetrated, proceed with steps 4-7. If penetration of more than one segment is indicated by the above check, a decision must be made as to the master segment to which the slave node is to be moved. In the current procedure, the normal projection of the slave node onto each candidate segment is computed. The slave node is then repositioned onto the master segment that results in the minimum change to its kinetic energy. Note that the maximum kinetic energy permitted by physical laws is the kinetic energy for unobstructed (i.e. nonintruding) slave node travel. This condition serves as an effective discriminant in selecting the appropriate master segment for relocation of the slave node.

4. If there is intrusion, position the slave node on the master segment in a direction normal to the segment.

5. Update master and slave node velocities to conserve linear and angular momentum.

6. Update nodal forces to account for change in nodal velocities.

7. At the option of the code user, interchange master and slave designations and repeat steps 1-6.

III. FINITE PLATE PERFORATION

Figure 1 shows results for the perforation of a 2.54cm armor steel plate by a 65 gram, hemispherically-nosed S-7 tool steel rod with a striking velocity of 1103 m/s. Figure 2 shows similar results for a plane strain simulation at an obliquity of 60^{o} and a striking velocity of 1647 m/s. Table 1 shows a comparison of computed residual masses and velocities with those obtained experimentally by Lambert[12] from radiographic data. The agreement is quite good for the normal impact case. The higher residual mass and velocity for the oblique impact case is characteristic of plane strain analyses due to differences in energy-displacement relationships for exact and plane strain formulation of computational elements.[13]

IV. PENETRATION OF SEMI-INFINITE TARGETS

A number of calculations with effectively semi-infinite targets struck by long rods (L/D = 10) at velocities of 1550, 2560, 3114, and 3750 m/s were also performed and compared with experimental data published by Hohler and Stilp.[14] The rods were made of C110W2 steel, had a diameter, D, of 0.43cm, length, L, of 4.3cm and density of 7.85 g/cc. The target material was HzB20 armor steel. In both calculations and experiments, the projectile was totally consumed. Also in both cases, the target thickness was at least twice the expected penetration depth. Figure 3 summarizes the initial conditions.

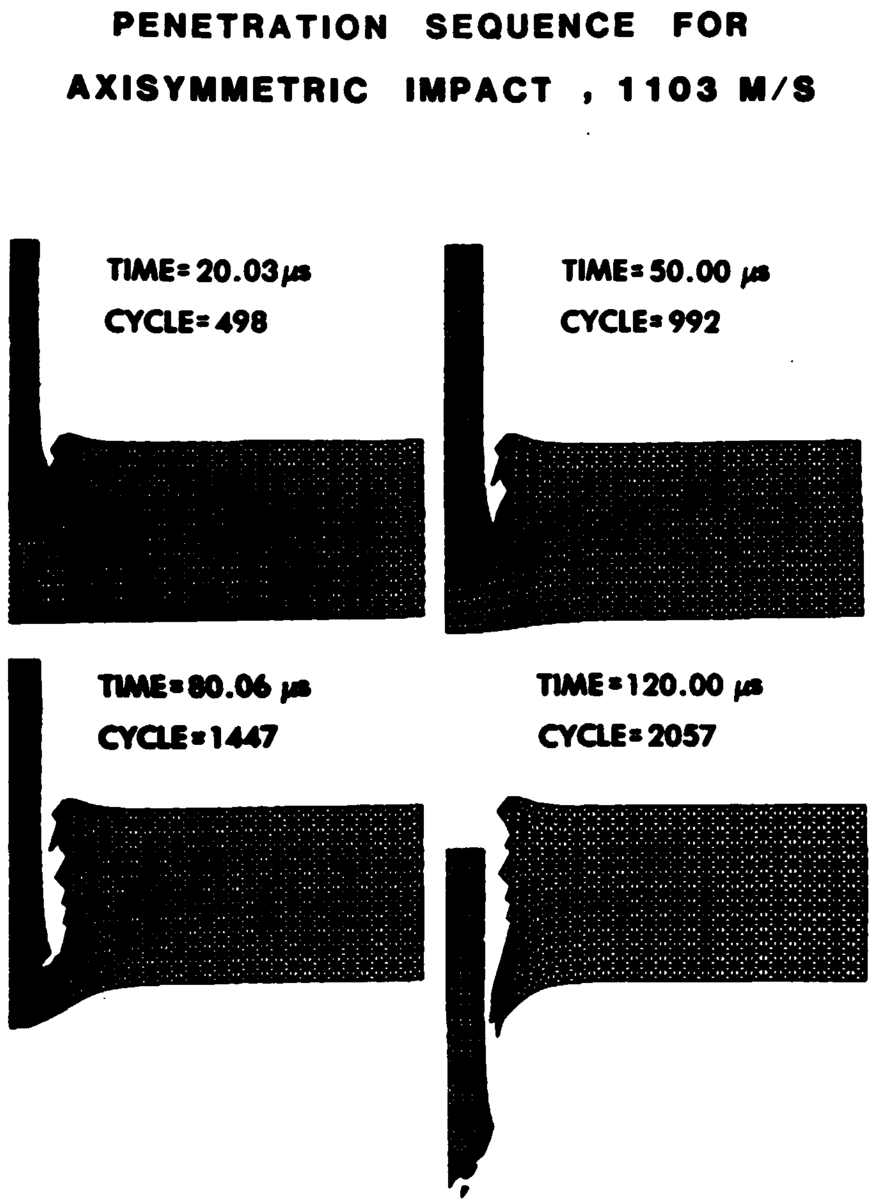

Figure 1. Deformation Profiles for Normal Penetration of Finite Target

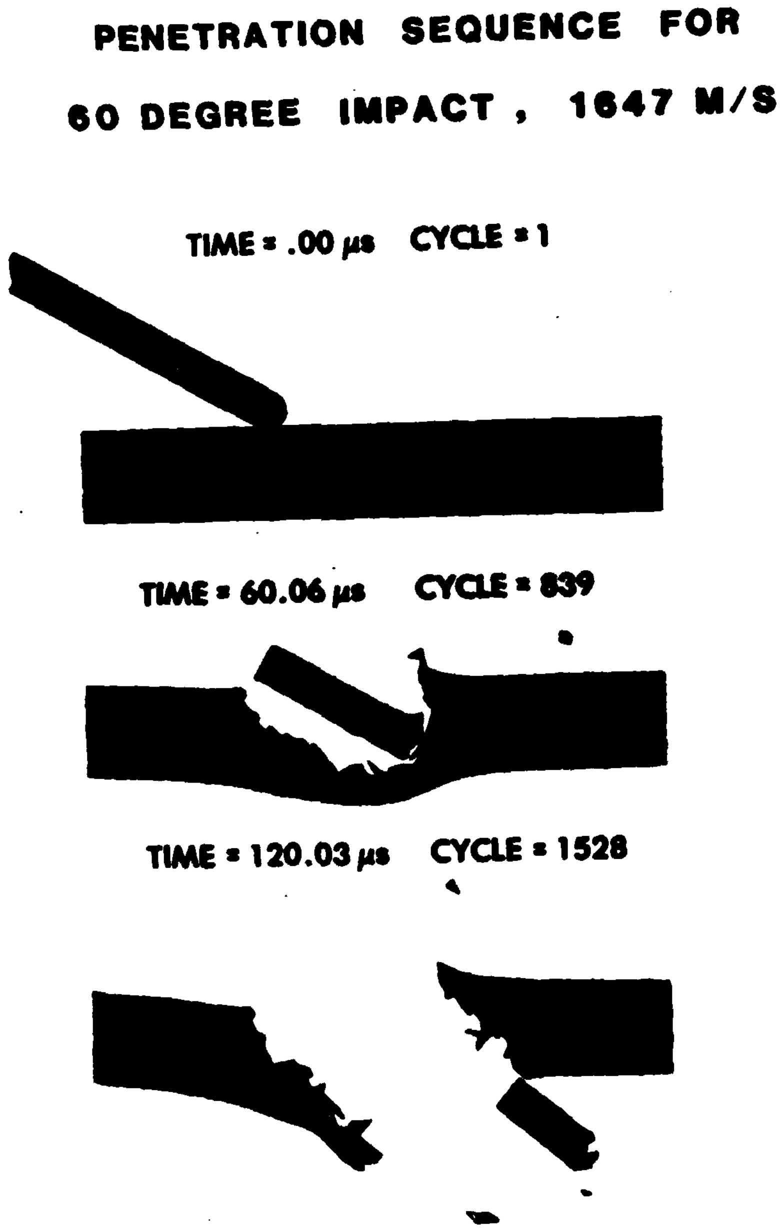

Figure 2. Plane Strain Results for Oblique Perforation of Finite Target

PENETRATION OF SEMI - INFINITE TARGETS

PROJECTILE: C110W2 STEEL

L/D 10

L 4.3 CM

7.85 GRAMS/CC

TARGET: HZB20 ARMOR STEEL

BHN 260 - 330 KP/ SQ. MM

SOUND VELOCITY, C 5950 M/S

Figure 3. Initial Conditions for Semi-infinite Target Penetration Study

Table 1. Results for Finite Target Penetration

CALCULATED AND MEASURED RESIDUAL PARAMETERS

L/D = 10 65 grams D = 1.0cm

θ	V_s (m/s)	Residual Velocity (m/s)		Residual Mass (g)	
		Calculated	Measured *	Calculated	Measured *
0°	1219	925	910	34.5	39.1 **
0°	1103	709	690	32.1	32.7
60°	1647	1202	1145	22.9	16.8

* *Ref: ARBRL - TR - 02072, May 1978*

** *Estimated from radiograph*

Results for the 3114 m/s impact condition are shown in Figures 4-7. Computed normalized penetration depth and crater diameter are compared with data from Hohler and Stilp[14] in Table 2 and Figures 8-10.

The computed values for penetration depth and crater diameter in Table 2a were obtained using the static material properties for projectile and target given in reference 14. Table 2b shows results using high strain rate data for the steel target obtained from Meyer's dissertation[15] with projectile strengths taken from reference 14. Both Table 2 and Figures 8-10 use computed values at the time when the projectile has been totally consumed (~45 μs for $v/c = 0.26$, between 22-30 μs for the remaining cases). Agreement with experimental results is generally good, except for the lowest striking velocity. In this regime, the impact response of materials is very strongly influenced by material strength. Evidently high strain rate data for the projectile material are required here, as well as a better material description (an **elastic, perfectly-plastic model was used throughout). As** striking velocity increases the influence of material strength decreases and agreement with experiment improves. The rather large overprediction of penetration depth at $v/c = 0.26$ (1550 m/s) using quasi-static ($\sim 10^{-4}$/s) data clearly suggests that dynamic characterization of materials is a **necessary** adjunct to impact experiments and code calculations in the ordnance velocity (0.5 - 2 km/s) regime.

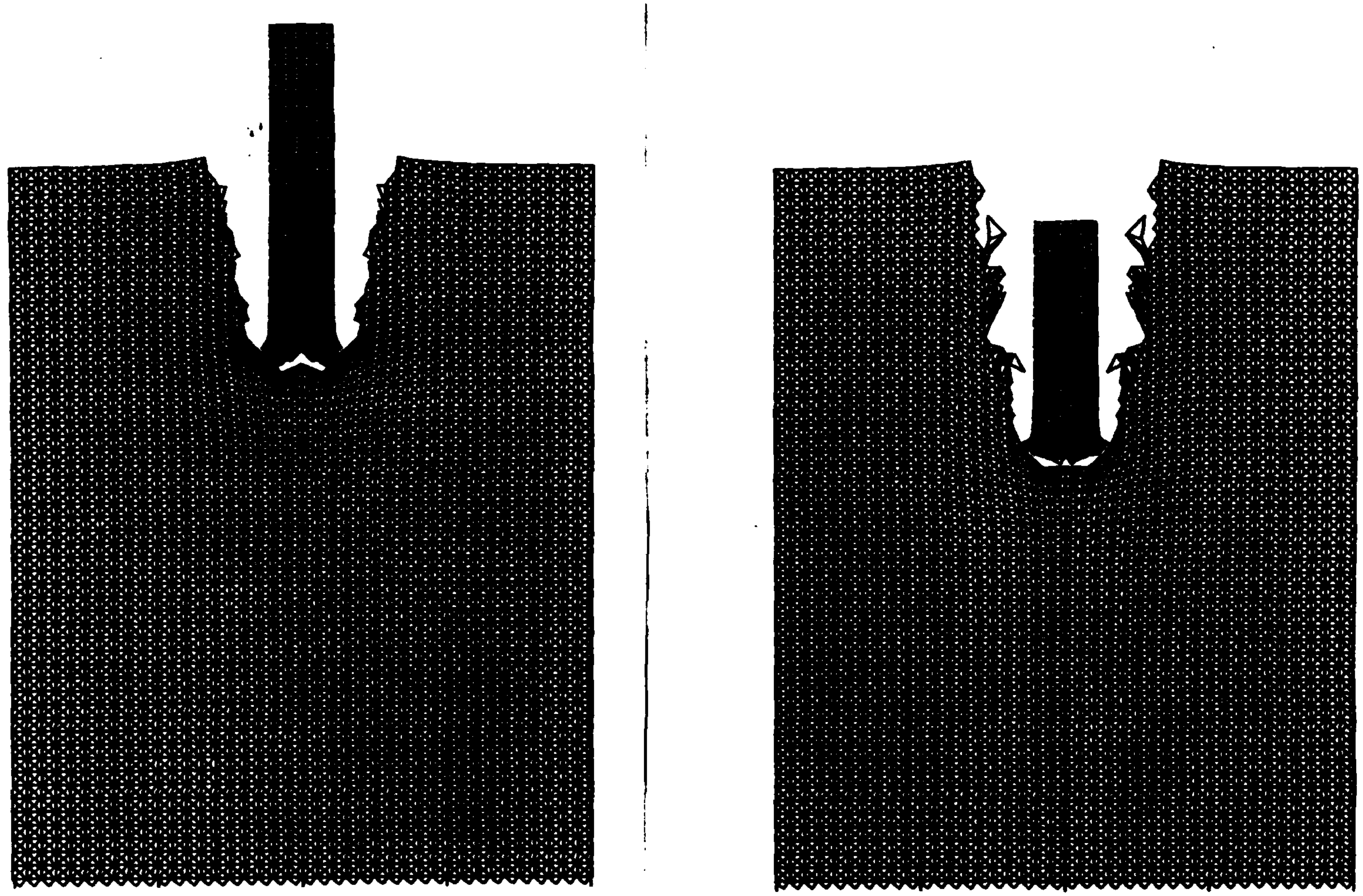

Figure 4. Deformation at 10 and 15 Microseconds after Impact

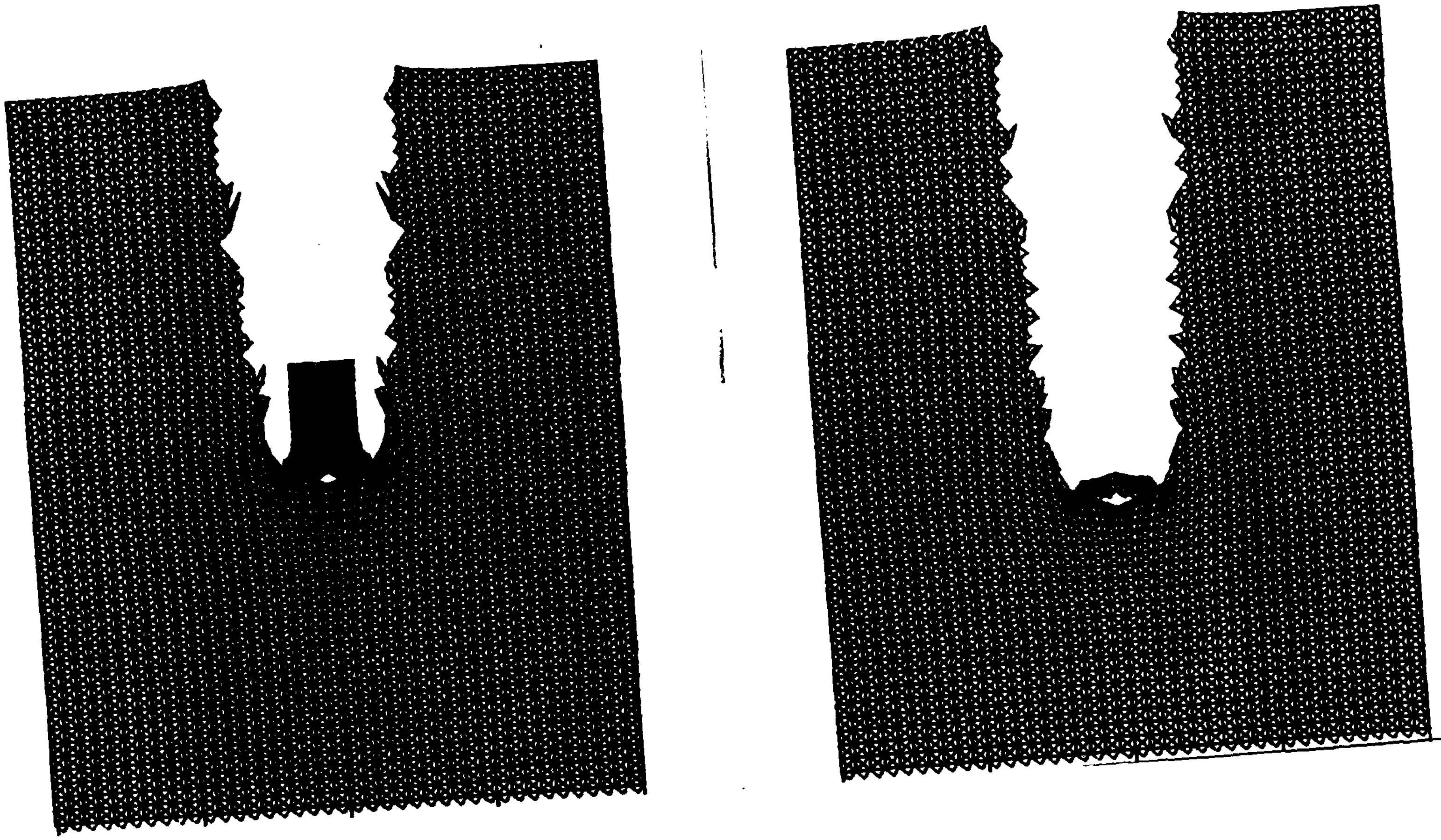

Figure 5. Deformation at 20 and 24 Microseconds after Impact

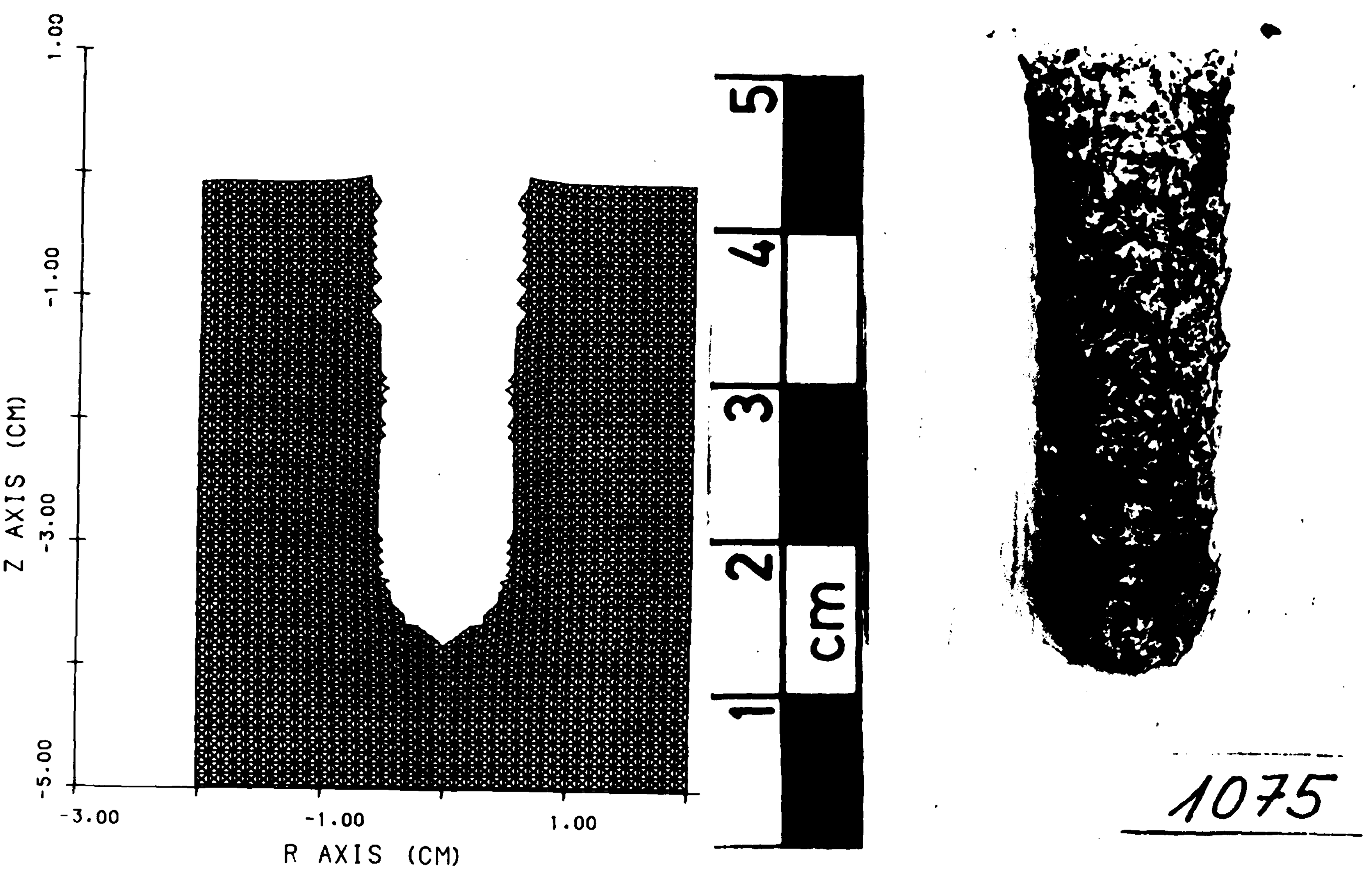

Figure 6. Computed (at 100 Microseconds after Impact) and Experimental Hole Profiles

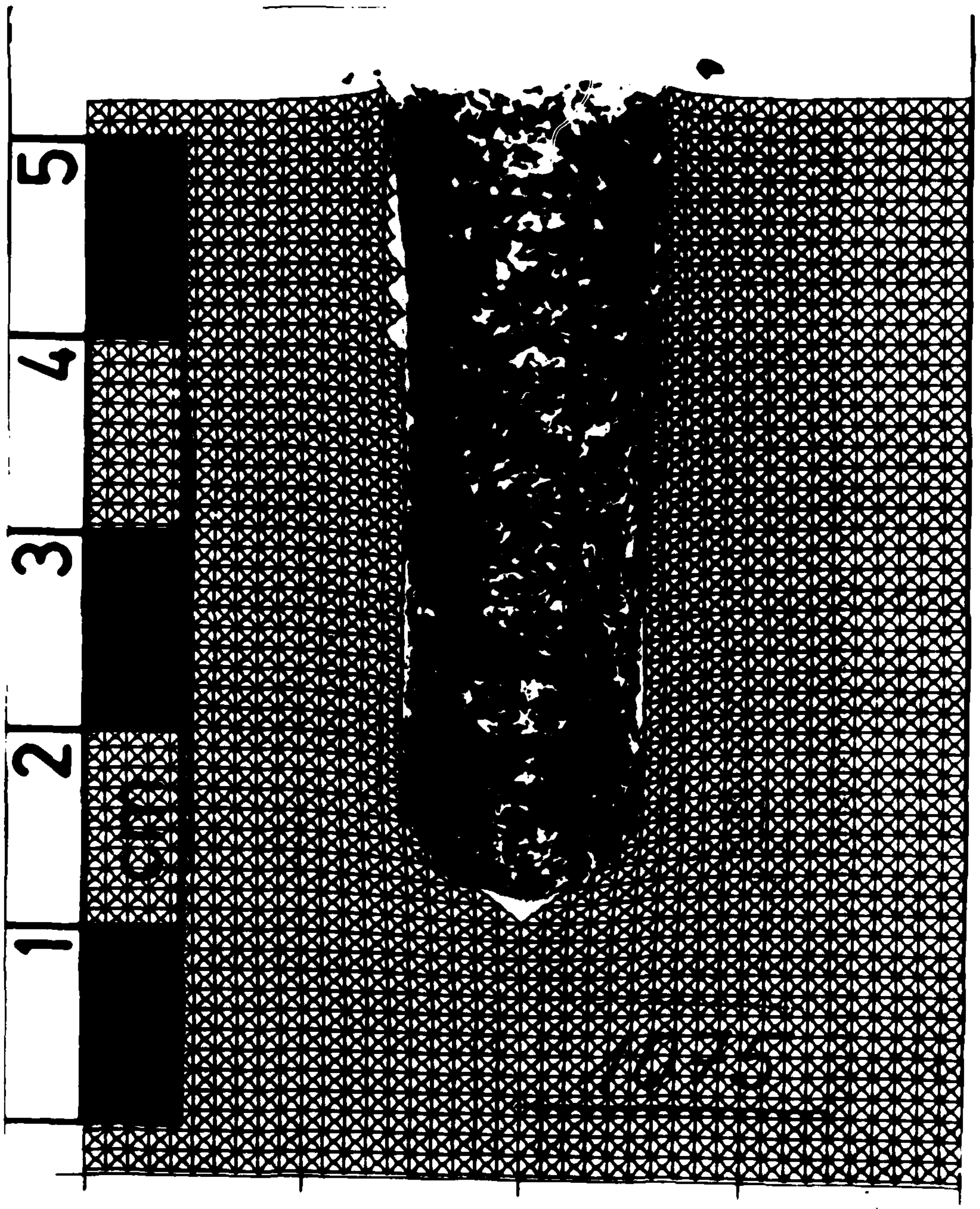

Figure 7. Overlay of Computed and Experimental Hole Profiles, vs = 3.114 km/s

Table 2a. Comparison of Calculated and Measured Residual Parameters for Penetration of Semi-Infinite Targets

v/c	P/L EXP (±0.06)	P/L CODE	P/d EXP (±0.15)	P/d CODE	d/D EXP	d/D CODE
0.26	0.33	0.58	1.5	2.5	2.2	2.3
0.43	0.80	0.86	2.9	3.0	2.7	2.8
0.52	0.90	0.91	3.0	3.0	3.0	3.1
0.63	0.93	0.93	2.7	2.8	3.5	3.3

Table 2b. Computations Using Dynamic Strength Data for the Target Material

v/c	P/L EXP (±0.06)	P/L CODE	P/d EXP (±0.15)	P/d CODE	d/D EXP	d/D CODE
0.26	0.33	0.40	1.5	1.8	2.2	2.3
0.43	0.80	0.75	2.9	2.9	2.7	2.8
0.52	0.90	0.85	3.0	3.0	3.0	3.0
0.63	0.93	0.88	2.7	2.8	3.5	3.3

Projectile

L = 4.3 cm
MATL = C110W2 steel
D = 0.43 cm
= 7.85 g/cc

Target

HzB20
BHN = 260-330 kp/mm^2

NOTES: P = penetration depth
d = crater diameter
v = projectile striking velocity
c = sound velocity for HzB20 (5950 m/s)

At the time the projectile is totally consumed, sufficient energy is trapped in the target to permit additional hole growth. Specifically, compressive pressures well in excess of the static or dynamic yield strength are to be found at the base of the crater at the time of total projectile erosion. Once the projectile is totally consumed a free surface at the crater base is created. The large compressive pressures will become tensile to satisfy this new boundary condition and will cause additional material failure until pressures and stresses fall below the material strength (this will

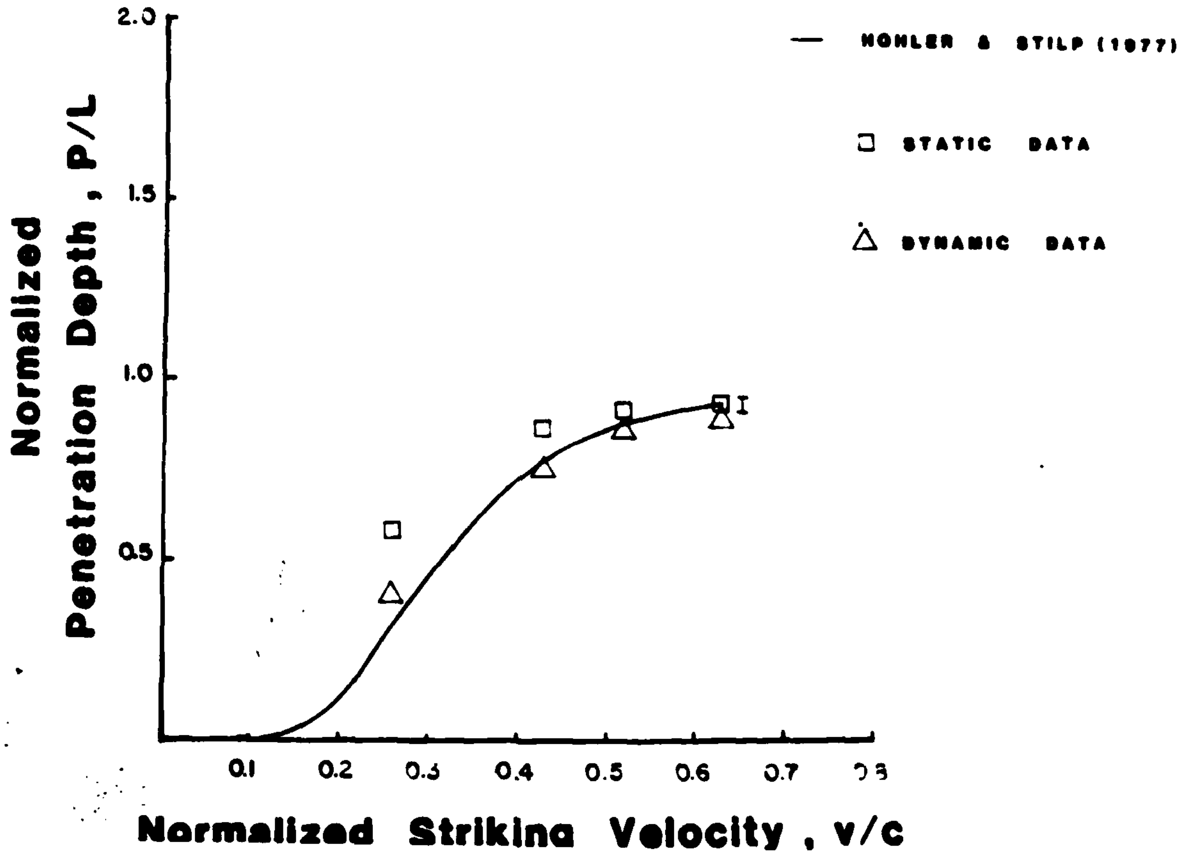

Figure 8. Comparison of Computed and Experimental Normalized Penetration Depth (P/L) vs Normalized Striking Velocity (v/c)

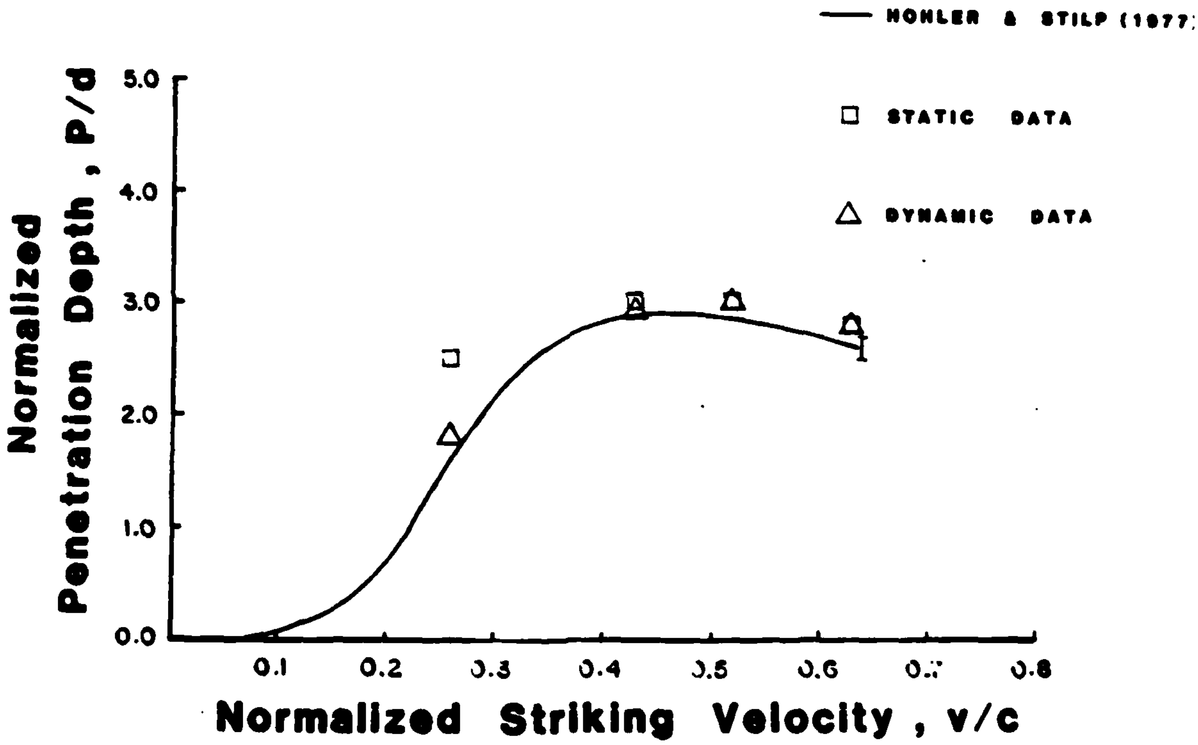

Figure 9. Comparison of Computed and Experimental Normalized Penetration Depth (P/d) vs Normalized Striking Velocity (v/c)

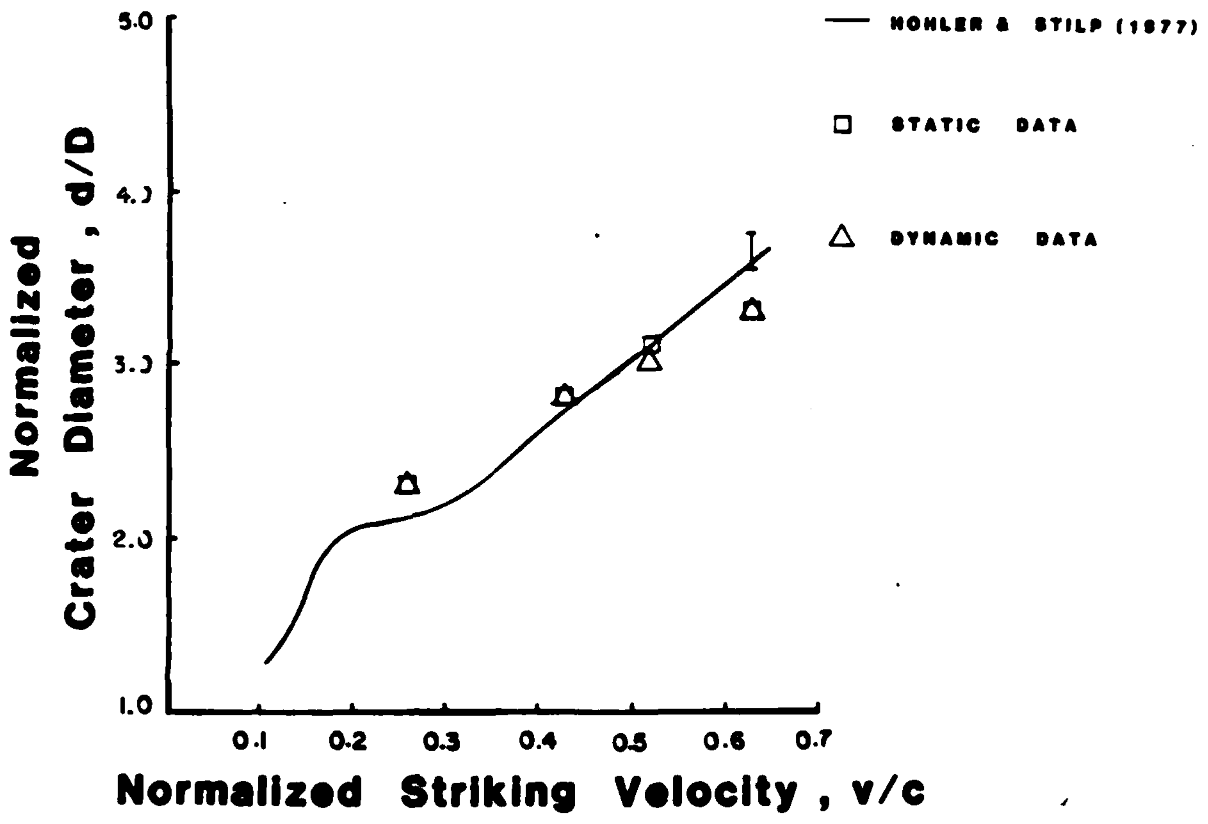

Figure 10. Comparison of Computed and Experimental Normalized Crater Diameter (d/D) vs Normalized Striking Velocity (v/c)

typically occur between 80-100 μs for all cases studied). The extent of this growth is shown in Table 3 which compares the experimentally measured (non-dimensionalized) penetration depth and hole diameter with those obtained computationally (using data from reference 15 for the target material) at a time when the projectile is totally consumed and also at 100 μs after impact. Changes in the diameter are negligibly small while hole growth is on the order of 3-5%.

Table 3. Residual Hole Growth

v/c	$(P/L)_{t1}$	$(P/L)_{t2}$	$(P/L)_{EXP}$	$(d/D)_{t1}$	$(d/D)_{t2}$	$(d/D)_{EXP}$
0.26	0.40	0.45	0.33	2.30	2.33	2.3
0.43	0.75	0.80	0.80	2.80	2.80	2.8
0.52	0.85	0.89	0.90	3.0	3.0	3.0
0.63	0.88	0.97	0.93	3.3	3.2	3.3

Note: t_1 = time at which projectile is totally consumed. For v/c of 0.26, 0.43, 0.52 and 0.63. This occurs at 45, 32, 26 and 22 μs respectively.

t_2 = 100 μs (time at which stresses & pressures are below target material yield strength).

V. CONCLUSIONS

The simulation of contact surface erosion in Lagrangian analyses of high velocity impacts appears to be a most promising refinement which extends the capabilities of Lagrangian codes for problems involving perforation of solids. The methodology permits simulation of deep penetration which previously was limited to Eulerian codes. Furthermore, the methodology has been demonstrated to yield residual parameters that are in good agreement with experimental data at a considerable reduction in CPU time and memory requirements for a comparable Eulerian analysis.

REFERENCES

1. J. A. Zukas, G. H. Jonas, K. D. Kimsey, J. J. Misey, and T. M. Sherrick, "Three-Dimensional Impact Simulations: Resources and Results," in K. C. Park and R. F. Jones, Jr., eds., Computer Analysis of Large-Scale Structures, AMD, Vol. 49, American Society of Mechanical Engineers, 1981.

2. A. Poth, et al., "Experimental and Numerical Investigation of the Ricochetting of Projectiles from Metallic Surfaces," Proceedings of the Sixth International Symposium on Ballistics, Joseph E. Backofen, Jr., ed., American Defense Preparedness Association, October 1981.

3. A. Poth, et al., "Failure Behavior of an Aluminum Plate Under Impact Loading," Proceedings of the International Conference on Application of Fracture Mechanics to Materials and Structures, Freiburg, West Germany, 1983.

4. R. Schwartz, et al., "Analysis of Reinforced Concrete Structures Subjected to Aircraft Impact Loading," Proceedings of the Seventh International Conference on Structural Mechanics in Reactor Technology, Chicago, Illinois, 1983.

5. G. R. Johnson, et al., "Three Dimensional Computer Code for Dynamic Response of Solids to Intense Impulsive Loads," International Journal for Numerical Methods in Engineering, Vol. 14, No. 12, 1979.

6. G. R. Johnson, et al., "Lagrangian Computations for Projectile Penetration into Thick Plates," to appear in Applied Computer Methods in Ballistics session at the 1984 ASME International Computers in Engineering Conference and Exhibit, Las Vegas, Nevada, August 12-16, 1984.

7. P. Snow, "KEPIC-2," Kaman Sciences Corporation Report K82-46U (R), August, 1982.

8. T. Belytschko and J. I. Lin, "A New Interaction Algorithm with Erosion for EPIC-3," BRL-CR-540, Feb 1985. Ballistic Research Laboratories Contract Report.

9. J. O. Hallquist, "A Numerical Treatment of Sliding Interfaces and Impact," in K. C. Park & D. K. Gartling, eds., Computational Techniques for Interface Problems, AMD Vol. 30, ASME, New York, 1978.

10. J. O. Hallquist, "A Numerical Procedure for Three-Dimensional Impact Problems," Preprint 2956, ASCE, October 1977.

11. G. R. Johnson, "EPIC-2, A Computer Program for Elastic-Plastic Impact Computations in 2 Dimensions Plus Spin," Ballistic Research Laboratory Contract Report No. ARBRL-CR-00373, June 1978.

12. J. P. Lambert, "The Terminal Ballistics of Certain 65 Gram Long Rod Penetrators Impacting Steel Armor Plate," Ballistic Research Laboratory Report No. ARBRL-TR-02072, May 1978.

13. J. A. Zukas, et al., "On the Utility of Plane Strain Approximations for Oblique Impact Computations," Ballistic Research Laboratory Report No. ARBRL-MR-02969, October 1979.

14. V. Hohler and A. J. Stilp, "Penetration of Steel and High Density Rods in Semi-Infinite Steel Targets," Proc. 3rd International Symposium on Ballistics, Karlsruhe, W. Germany, 1977.

15. L. W. Meyer, Thesis No. 81/106, University of Dortmund, West Germany, 1982.

DISTRIBUTION LIST

No. of Copies	Organization
12	Administrator Defense Technical Info Center ATTN: DTIC-DDA Cameron Station Alexandria, VA 22314
1	Director Defense Advanced Research Projects Agency ATTN: Dr. W. Snowden 1400 Wilson Boulevard Arlington, VA 22209
1	Director Defense Nuclear Agency Arlington, VA 22209
1	Deputy Assistant Secretary of the Army (R&D) Department of the Army Washington, DC 20310
2	Commander US Army BMD Advanced Technology Center ATTN: BMDATC-M, Mr. P. Boyd Mr. S. Brockway PO Box 1500 Huntsville, AL 35807
1	HQDA (DAMA-ARP) WASH DC 20310
1	HQDA (DAMA-MS) WASH DC 20310
2	Commander US Army Engineer Waterways Experiment Station ATTN: Dr. P. Hadala Dr. B. Rohani PO Box 631 Vicksburg, MS 39180
1	Commander US Army Materiel Command ATTN: DRCDMD-ST 5001 Eisenhower Avenue Alexandria, VA 22333

No. of Copies	Organization
4	Commander US Army Research and Development Center ATTN: DRSMC-LCU(D), E. Barrieres DRSMC-SCM(D), Dr.E. Bloore DRSMC-TSS (2 cys) Dover, NJ 07801
2	Director US Army AMCCOM Benet Weapons Laboratory ATTN: DRSMC-LCB-TL Dr. Joseph E. Flaherty Watervliet, NY 12189
1	Commander US Army Armament Materiel Readiness Command ATTN: DRSAR-LEP-L, Tech Lib Rock Island, IL 61299
1	Commander US Army Aviation Research and Development Command ATTN: DRDAV-E 4300 Goodfellow Blvd. St. Louis, MO 63120
1	Director US Army Air Mobility Research and Development Laboratory Ames Research Center Moffett Field, CA 94035
1	Commander US Army Communications Research and Development Command ATTN: DRSEL-ATDD Fort Monmouth, NJ 07703
1	Commander US Army Electronics Research and Development Command Technical Support Activity ATTN: DELSD-L Fort Monmouth, NJ 07703

DISTRIBUTION LIST

No. of Copies	Organization
3	Commander US Army Missile Research and Development Command ATTN: DRSMI-R DRSMI-RBL DRSMI-YDL Redstone Arsenal, AL 35809
2	Commander US Army Tank-Automotive Research and Development Command ATTN: DRDTA-UL V. H. Pagano Warren, MI 48090
1	Commander TARADCOM Tank-Automotive Systems Laboratory ATTN: T. Dean Warren, MI 48090
6	Director US Army Material Technology Laboratory ATTN: DRXMR-T Mr. J. Mescall Dr. M. Lenoe R. Shea F. Quigley DRXMR-ATL Watertown, MA 02172
2	Commander US Army Research Office ATTN: Dr. E. Saibel Dr. G. Mayer PO Box 12211 Research Triangle Park NC 27709
1	Director US Army TRADOC Systems Analysis Activity ATTN: ATAA-SL (Tech Lib) White Sands Missile Range NM 88002
1	Commander Naval Air Systems Command ATTN: AIR-604 Washington, DC 20360

No. of Copies	Organization
1	Commander Naval Ordnance Systems Command Washington, DC 20360
1	Commander Naval Air Development Center, Johnsville Warminster, PA 18974
1	Commander Naval Missile Center Point Mugu, CA 93041
2	Naval Ship Engineering Center ATTN: J. Schell Tech Lib Washington, DC 20362
1	Commander & Director David W. Taylor Naval Ship Research & Development Center ATTN: Code 1740.4, R. A. Gramm Bethesda, MD 20084
3	Commander Naval Surface Weapons Center ATTN: Dr. W. G. Soper Mr. N. Rupert Code G35, D. C. Peterson Dahlgren, VA 22448
10	Commander Naval Surface Weapons Center ATTN: Code R-32 Alexander Rozner Hampton de Jarnette Code U-23 William Hinckley Code R-13, F. J. Zerilli K. Kim E. T. Toton M. J. Frankel Code U-11, J. R. Renzi R. S. Gross Code K-22, J. Etheridge Silver Spring, MD 20903-5000

DISTRIBUTION LIST

No. of Copies	Organization
3	Commander Naval Weapons Center ATTN: Code 31804, Mr. M. Smith Code 326, Mr. P. Cordle Code 3261, Mr. T. Zulkoski China Lake, CA 93555
7	Commander Naval Weapons Center ATTN: Code 3181, John Morrow Code 3261, Mr. C. Johnson Code 3171, Mr. B. Galloway Code 3831, Mr. M. Backman Dr. O. E. R. Heimdahl Dr. Kenneth Graham Code 3894, C. Lorenzen China Lake, CA 93555
1	Director Naval Research Laboratory ATTN: Dr. C. Sanday Washington, DC 20375
3	Superintendent Naval Postgraduate School ATTN: Dir of Lib Dr. Gilbert Kinney Dr. Richard Reinhardt Monterey, CA 93940
1	HQ USAF/SAMI Washington, DC 20330
1	AFIS/INOT Washington, DC 20330
3	ADTC/DLJW (LT K. Ols, LT J. Flores, Mr. W. Cook) Eglin AFB, FL 32542
1	ADTC/DLYV (Mr. J. Collins) Eglin AFB, FL 32542
1	AUL-LSE 71-249 Maxwell AFB, AL 36112

No. of Copies	Organization
1	AFWAL/MLLN (Dr. T. Nicholas) Wright-Patterson AFB, OH 45433
4	Lawrence Livermore National Laboratory PO Box 808 ATTN: Tech Library Dr. J. O. Hallquist Dr. M. L. Wilkins Dr. G. Goudreau Livermore, CA 94550
7	Los Alamos Scientific Laboratory PO Box 1663 ATTN: Dr. R. Karpp Dr. J. Dienes Dr. J. Taylor John Meier Scott Hill Dr. C. Mader Tech Library Los Alamos, NM 87545
9	Sandia National Laboratories ATTN: Dr. R. Woodfin Dr. M. Sears Dr. W. Herrmann Dr. A. Chabai M. Kipp T. Burns A. L. Stevens M. J. Forrestal M. J. Sagartz L. Davison Albuquerque, NM 87115
2	Sandia National Laboratories ATTN: Dr. L. D. Bertholf Dr. D. Bammann Livermore, CA 94550
1	Headquarters National Aeronautics and Space Administration Washington, DC 20546
1	US Geological Survey 2255 N. Gemini Drive ATTN: Dr. D. Roddy Flagstaff, AZ 86001

DISTRIBUTION LIST

No. of Copies	Organization
1	AAI Corporation PO Box 6767 ATTN: R. L. Kachinski Baltimore, MD 21204
1	AVCO Systems Division 201 Lowell Street ATTN: Dr. Reinecke Wilmington, MA 01803
1	Battelle Columbus Laboratories 505 King Avenue ATTN: G. Throner Columbus, OH 43201
4	Boeing Aerospace Company ATTN: Mr. R. G. Blaisdell (M.S. 40-25) Dr. N. A. Armstrong, C. J. Artura (M.S. 8C-23) Dr. B. J. Henderson (M.S. 43-12) Seattle, WA 98124
1	Computer Code Consultants, Inc. 1680 Camino Redondo ATTN: Dr. Wally Johnson Los Alamos, NM 87544
1	Electric Power Research Institute PO Box 10412 ATTN: Dr. George Sliter Palo Alto, CA 94303
4	FMC Corporation Ordnance Engineering Division ATTN: Neil Kennedy Claude Braafladt Robert Burt Anthony Lee PO Box 1201 San Jose, CA 95108
4	Ford Aerospace and Communications Corporation Ford Road, PO Box A ATTN: L. K. Goodwin C. E. Blair E. R. Mijares R. C. Morenus Newport Beach, CA 92660
1	General Dynamics PO Box 2507 ATTN: J. H. Cuadros Pomona, CA 91745
1	General Electric Company Lakeside Avenue ATTN: D. Graham, Rm 1311 Burlington, VT 05401
1	H. P. White Laboratory 3114 Scarboro Road Street, MD 21154
5	Honeywell, Inc. ATTN: Mr. J. Blackburn Dr. G. Johnson Mr. K. H. Doeringsfeld Dr. C. Candland Ms. Peggy Anderson 5901 South County Road 18 Edina, MN 55436
1	Lockheed Missiles & and Space Co. PO Box 3504 ATTN: Org 8320, Bldg 157-3W Robert Weinheimer Sunnyvale, CA 94088-3504
2	Lockheed Missiles and Space Company PO Box 504 ATTN: R. L. Williams Dept 81-11, Bldg 154 Robert Cothern Dept 86-54, Bldg 153 Sunnyvale, CA 94086

DISTRIBUTION LIST

No. of Copies	Organization
1	Materials Research Laboratory, Inc. 1 Science Road Glenwood, IL 60427
2	McDonnell-Douglas Astronautics Company 5301 Bolsa Avenue ATTN: Dr. L. B. Greszczuk Dr. J. Wall Huntington Beach, CA 92647
3	New Mexico Institute of Mining and Technology ATTN: Lamar Kempton Dr. Max Bloom Dr. M. A. Meyer Socorro, NM 87801
2	Orlando Technology, Inc. PO Box 855 ATTN: Mr. J. Osborn Mr. D. Matuska Shalimar, FL 32579
1	Pacific Technical Corporation 460 Ward Drive ATTN: Dr. F. K. Feldmann Santa Barbara, CA 93105
1	Rockwell International Missile Systems Division ATTN: A. R. Glaser 4300 E. Fifth Avenue Columbus, OH 43216
3	Schumberger Well Services Perforating Center ATTN: J. E. Brooks J. Brookman Dr. C. Aseltine PO Box A Rosharon, TX 77543

No. of Copies	Organization
6	Strategic Defense Initiative Organization 1717 H Street, NW ATTN: Dr. Gerold Jones, Rm 416 Dr. James Ionson, Rm 326 COL Malcolm O'Neill, Rm 734 Dr. Louis Marquet, Rm 331 Mr. John Gardner, Rm 332 COL George Hess, Rm 449 Washington, DC 20006
1	Systems, Science and Software PO Box 1620 ATTN: Dr. R. Sedgwick La Jolla, CA 92038
2	TRW One Space Park, R1/2120 ATTN: D. Ausherman M. Bronstein Redondo Beach, CA 90277
1	United Technologies Research Center 438 Weir Street ATTN: P. R. Fitzpatrick Glastonbury, CT 06033
1	US Steel Corporation Research Center 125 Jamison Center Monroeville, PA 15146
2	Vought Corporation PO Box 225907 ATTN: Dr. G. Hough Dr. Paul M. Kenner Dallas, TX 75265
1	Drexel University Department of Mechanical Engr. ATTN: Dr. P. C. Chou 32d and Chestnut Streets Philadelphia, PA 19104

DISTRIBUTION LIST

No. of Copies	Organization
4	Southwest Research Institute Dept. of Mechanical Sciences ATTN: Dr. U. Lindholm Dr. R. White Dr. M. F. Kanninen Dr. C. Anderson 8500 Culebra Road San Antonio, TX 78228
4	SRI International 333 Ravenswood Avenue ATTN: Dr. L. Seaman Dr. L. Curran Dr. D. Shockey Dr. A. L. Florence Menlo Park, CA 94025
2	University of Arizona Civil Engineering Department ATTN: Dr. D. A. DaDeppo Dr. R. Richard Tucson, AZ 85721
2	University of California College of Engineering ATTN: Prof. W. Goldsmith Dr. A. G. Evans Berkeley, CA 94720
4	University of Delaware Department of Mechanical Engineering ATTN: Prof. J. Vinson Prof. B. Pipes Prof. M. Taya Prof. T-Y Chou Newark, DE 19711
1	University of Denver Denver Research Institute ATTN: Mr. R. F. Recht 2390 S. University Blvd. Denver, CO 80210
1	University of Florida Department of Engineering Sciences ATTN: Dr. L. E. Malvern Gainesville, FL 32601

No. of Copies	Organization
	<u>Aberdeen Proving Ground</u>
	Dir, USAMSAA ATTN: DRXSY-D DRXSY-MP, H. Cohen Cdr, USATECOM ATTN: DRSTE-TO-F Dir, USAAPG ATTN: Mr. W. Pless, MTD Mr. S. Keithely, MTD Dir, USACSL, EA ATTN: DRSMC-CLB-PA Bldg. E3516
10	Central Intelligence Agency Office of Central Reference Dissemination Branch Room GE-47 HQS Washington, D.C. 20502

USER EVALUATION SHEET/CHANGE OF ADDRESS

This Laboratory undertakes a continuing effort to improve the quality of the reports it publishes. Your comments/answers to the items/questions below will aid us in our efforts.

1. BRL Report Number________________ Date of Report________

2. Date Report Received________________

3. Does this report satisfy a need? (Comment on purpose, related project, or other area of interest for which the report will be used.)________

4. How specifically, is the report being used? (Information source, design data, procedure, source of ideas, etc.)________

5. Has the information in this report led to any quantitative savings as far as man-hours or dollars saved, operating costs avoided or efficiencies achieved, etc? If so, please elaborate.________

6. General Comments. What do you think should be changed to improve future reports? (Indicate changes to organization, technical content, format, etc.)

CURRENT ADDRESS

Name

Organization

Address

City, State, Zip

7. If indicating a Change of Address or Address Correction, please provide the New or Correct Address in Block 6 above and the Old or Incorrect address below.

OLD ADDRESS

Name

Organization

Address

City, State, Zip

(Remove this sheet along the perforation, fold as indicated, staple or tape closed, and mail.)

— — — — — — — — — — FOLD HERE — — — — — — — — — — —

Director
U.S. Army Ballistic Research Laboratory
ATTN: SLCBR-DD-T
Aberdeen Proving Ground, MD 21005-5066

NO POSTAGE NECESSARY IF MAILED IN THE UNITED STATES

OFFICIAL BUSINESS
PENALTY FOR PRIVATE USE, $300

BUSINESS REPLY MAIL
FIRST CLASS PERMIT NO 12062 WASHINGTON, DC

POSTAGE WILL BE PAID BY DEPARTMENT OF THE ARMY

Director
U.S. Army Ballistic Research Laboratory
ATTN: SLCBR-DD-T
Aberdeen Proving Ground, MD 21005-9989

— — — — — — — — — — FOLD HERE — — — — — — — — — — —